Progress In Electromagnetics Research C, Vol. 64, 79–87, 2016

Novel X-Band Waveguide Dual Circular Polarizer

Chen Xu*, Sami Tantawi, and Juwen Wang

Abstract—Novel types of dual circular polarizer are developed to convert TE10 mode into two different polarized TE11 modes in a circular waveguide. These designs have MHz bandwidth and high power transmission capability.They can be used for broadcasting and receiving circular polarized signals.

1. INTRODUCTION

X-band microwave orthomode transducer (OMT) is widely used for different experiments such as cosmic microwave background polarization experiment [1]. Transducer can broadcast RF wave energy in the form of two TE11 modes which share the same frequency but at 90 degrees' orientation polarizations. Such a device can convert input RF energy from a RF source and split RF energy into two polarized modes in a circular waveguide [2–4]. Generally speaking, TE10 mode, which is the lowest frequency mode in a given rectangular waveguide, can be easily obtained from a klystron. On the other hand, the OMT can also receive reflection signals from a cosmic emitter. The received signals contain RF energy, and these RF energies can be coupled to the two TE11 modes independently. OMT device can distribute the components of orthogonally polarized microwave signals into different rectangular waveguides [5, 6]. Examining the phases and amplitudes of the received signals, one can learn the emission RF characteristics [7–9]. With different purposes of the application, different types of OMT are designed and tested in SLAC [10, 11]. They may have different numbers of rectangular input ports. However, the designs utilize some isolated posts or rectangular blocks to ensure the RF matches and isolations between ports. Those additional geometries limit the maximum RF power and undermine the thermal instability, due to magnetic field enhancement [11]. Also, they will introduce manufactory difficulties. In this report, we propose a converter design which has no posts or other additional geometries. This three-ports OMT converter will convert input from one rectangular waveguide and output signals on the circular waveguide. The combined TE11 modes are left-hand circularly polarized (LHCP). LHCP mode reveals as one TE11 mode rotating clockwise because the phase delay between vertical and horizontal modes is 90 degrees. Meanwhile, both polarizations have the same amplitudes. If a received signal is right-hand circularly polarized (RHCP), it will output solely to the second rectangular waveguide on the other side. RHCP will have 270-degree difference between two polarizations. A diagram of the power flow is illustrated in Figure 1.

2. ANALYTICAL DESIGN METHODOLOGY

This device will have three physical ports, and the circular wave port supports two polarization modes. The RF energy will be converted among four modes. Thus a 4 by 4 scattering matrix will be studied for

Received 7 April 2016, Accepted 11 May 2016, Scheduled 18 May 2016
* Corresponding author: Chen Xu (chenxu@slac.stanford.edu).
The authors are with the SLAC National Accelerator Laboratory, Stanford University, Stanford, CA 94309, USA.

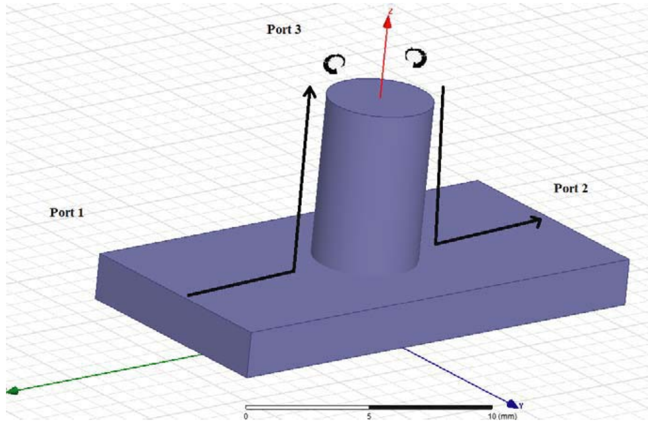

Figure 1. Demonstration design of circular polarizer and its power flow. TE10 mode in port1 will output LHCP signals on port 3. It can be used in a reverse way. Both polarizations of LHCP and RHCP have the same amplitude and the only different is the phase delay.

the RF mode conversion. To achieve the goal that we describe in Figure 1, the targeted core scattering matrix for these four modes should be the following:

$$S = \frac{1}{2} \times \begin{bmatrix} 0 & 0 & \sqrt{2} & -\sqrt{2}i \\ 0 & 0 & -\sqrt{2} & -\sqrt{2}i \\ \sqrt{2} & -\sqrt{2} & 0 & 0 \\ -\sqrt{2}i & -\sqrt{2}i & 0 & 0 \end{bmatrix} \tag{1}$$

where the first two modes are the TE10 modes on both end rectangular waveguides, and the last two modes are the two TE11 modes in the circular waveguide. This matrix is a unitary matrix.

When the RF power comes from port 1, it will be split equally into H polarization 1 and V polarization 2 in the fourth port, and those two modes have 90-degree phase difference. This is a LHCP mode. If the RF power comes from rectangular port 2, it will split equally into those two polarizations with 270 (or -90) degree delay. This is a RHCP mode. When the power received from port 3 has two modes with 180-degree phase difference, the power will be distributed equally to two rectangular ports. In any case, 2 rectangular waveguides are isolated.

Matrix 1 is a core matrix and simplified, because the phase of each mode can be different and depends on the length of the waveguides. One needs to cascade this core scattering matrix with a phase shift matrix. The phase shift matrix is related to the lengths of input and output waveguides. However, the phase shift matrix will not change amplitude and phase difference. Thus, there is a more general form of the transfer 4 by 4 matrix, it is shown as following.

$$S = \frac{1}{2} \times \begin{bmatrix} 0 & 0 & \sqrt{2} \times e^{-j\omega\left(\frac{L_1}{\beta_1}+\frac{L_3}{\beta_3}\right)} & -\sqrt{2}i \times e^{-j\omega\left(\frac{L_2}{\beta_2}+\frac{L_3}{\beta_3}\right)} \\ 0 & 0 & -\sqrt{2} \times e^{-j\omega\left(\frac{L_1}{\beta_1}+\frac{L_3}{\beta_3}\right)} & -\sqrt{2}i \times e^{-j\omega\left(\frac{L_2}{\beta_2}+\frac{L_3}{\beta_3}\right)} \\ \sqrt{2} \times e^{-j\omega\left(\frac{L_1}{\beta_1}+\frac{L_3}{\beta_3}\right)} & -\sqrt{2} \times e^{-j\omega\left(\frac{L_1}{\beta_1}+\frac{L_3}{\beta_3}\right)} & 0 & 0 \\ -\sqrt{2}i \times e^{-j\omega\left(\frac{L_2}{\beta_2}+\frac{L_3}{\beta_3}\right)} & -\sqrt{2}i \times e^{-j\omega\left(\frac{L_2}{\beta_2}+\frac{L_3}{\beta_3}\right)} & 0 & 0 \end{bmatrix} \tag{2}$$

The modes sequence is the same as that shown in matrix 1. In this matrix, L_1, L_2 and L_3 are the lengths of three arms, and $\beta_1\beta_2$ and β_3 are the propagation constants in each waveguide. In our case, β_1 and β_2 are the same, because we will use the same rectangular waveguide on both ends.

3. ANALYTICAL STUDY OF A SIMPLIFIED POLARIZER

How to split the RF energy and couple it to two different polarizations? One has to split the input power to two different modes. As mentioned above, the input power comes in a form of TE10 mode from a rectangular waveguide. The next lowest mode in the rectangular waveguide is TE20 mode [12]. At this moment, we presume that we convert TE10 into an over-moded TE10 and TE20 combination. We will address how to get this input in the later context. Now we have an input rectangular waveguide with TE10 and TE20 modes with equal amplitude and arbitrary phase difference. By doing this, we can separate this converter into two parts: a center unit which converts TE10/TE20 to two TE11 polarizations in circular waveguide, and an end unit which converts TE10 modes to TE10/TE20 combinations.

4. DESIGN OF THE CENTER UNIT

Now we design the center unit. Instead of three ports, this center piece will have two physical ports: one circular and one rectangular waveguide in Figure 2. Each port will support two modes. A short plate is added on one side of the circular waveguide. After examining the electromagnetic field patterns of TE10 and TE20 and TE11 in both waveguides, we find that TE10 can be easily coupled to TE11 vertical polarization, and TE20 can be coupled to TE11 horizontal polarization independently, because they are orthogonal modes.

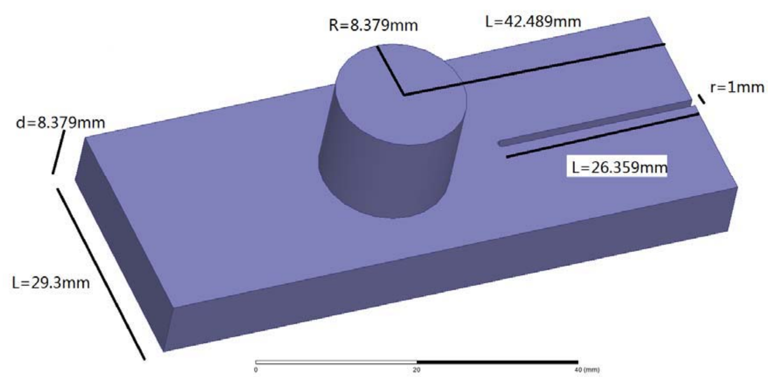

Figure 2. The geometry of the center convertor. The geometry dimensions are labeled.

Shown in Figure 2, we can form two standing wave modes between the shorting plate and circular waveguide. The standing wave modes are formed by TE010 and TE020 modes inputs. With correct distance between short plate and circular waveguide, both TE10 and TE20 modes from rectangular waveguide have perfect matches to two polarizations on the circular waveguide independently. To achieve this goal, the center device will have a 4 by 4 scattering matrix as following. The first two modes are TE10 and TE20 from rectangular waveguide and last two are TE11 modes on circular waveguide.

$$S = \begin{bmatrix} 0 & 0 & 1 \times e^{j\theta_1} & 0 \\ 0 & 0 & 0 & 1 \times e^{j\theta_2} \\ 1 \times e^{j\theta_1} & 0 & 0 & 0 \\ 0 & 1 \times e^{j\theta_2} & 0 & 0 \end{bmatrix} \tag{3}$$

where θ_1 and θ_2 are the phase delay for TE10 and TE20 modes in this structure.

As mentioned above, two standing wave modes will be coupled by the circular waveguide when their maximums H fields' location is just at the root of circular waveguide. The peak fields need to have the same amplitude and occur at the same location in order to achieve the requirement of LHCP or RHCP. In addition, we also need to make sure that two polarizations have −90-degree phase difference. To achieve these requirements, TE10 and TE20 modes are optimized individually since they are orthogonal and independent. The distance from the center of circular waveguide to the short end should be approximately half guided wavelength for each mode. But the guided wave lengths of TE10 and TE20 are not the same in a given rectangular waveguide. To solve this problem, a thin fin groove is added at the center of the shorted plate. The design of a convertor is shown in Figure 3. For TE10 mode conversion, shown in Figure 3(a), the fin acts like short end to TE10, because TE10 is too wide thus become evanescent mode at the fin tip. One the other hand, TE20 mode (Figure 3(b)) can propagate with little reflection in the fin area because TE20 has no field in the center. The length of the fin can be adjusted to move the peak E field of TE10 and TE20 to the same location. At this location, we add a circular waveguide port to achieve max extractions of both modes. Each mode will be fully matched to one TE11 polarization individually. A snap shot of E field in this convertor is shown in Figure 3(c). The simulations in this study are conducted in HFSS simulation [13]. A LHCP mode is formed at this setup in Figure 3(c).

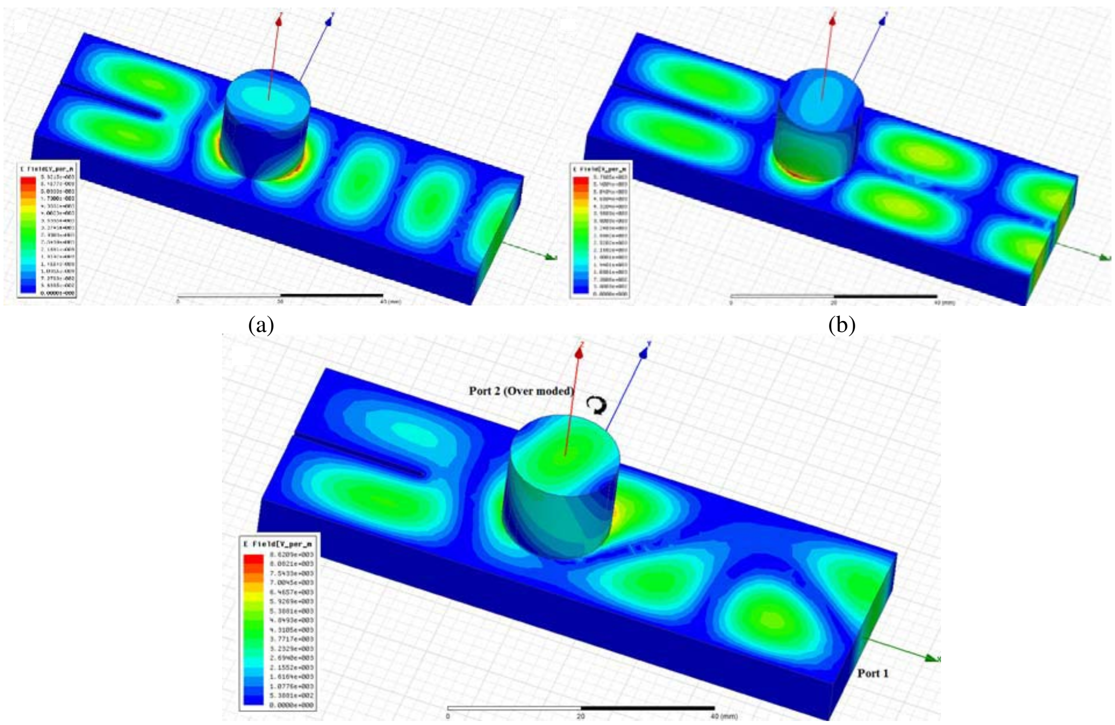

(a) (b)

(c)

Figure 3. This is the electric field patterns on the center converter First two figures are shown when input modes are single individual modes and last figure shows that a combination scenario. (a) TE10 conversion; (b) TE20 conversion; (c) a snap shot E field on converter with an over-moded input power. In these figures, the electric fields are plotted when the input powers on port1 are normalized to 1 W for each TE10/TE20 modes. The field amplitude increases quadratic when power increase linearly.

The output of circular waveguide is a combination of two polarized TE11 modes. The phase delay will determine if they form a RHCP or LHCP. If the delay is -90, they form a LHCP, and vice versa. The degree phase difference between θ_1 and θ_2 in matrix 3 can be adjusted by the input TE10 and TE20 initial phase difference at port 1. This initial phase can be changed by the length of a rectangular waveguide. Because TE10 and TE20 have different propagation constants, the phase difference can be any arbitrary number. In this case, adjusting the phase delay and amplitude are independent. At this moment, we focus on matching the amplitudes of both modes to the value in matrix 9 and leave θ_1 and θ_2 arbitrary numbers. After optimization, a 4 by 4 scattering-parameters matrix at 11.424 GHz is given in Table 1. The first two modes are TE10 and TE20 on port 1, and last two modes are two TE11 on port 2. Achieving this transfer matrix suggests that both modes are matched from port 1 to port 2 with minimal reflection to the input rectangular waveguide.

Table 1. The scattering matrix of device in Figure 3. The modes sequence is the same as shown in matrix 2. First number is amplitude and second number is phase delay from input port. $S : M : N$ means Nth mode on M port. First number is S parameter whose unit is decibel (dB) and second number is phase whose unit is degree.

Frequency: 11.424 GHz	S:1:1	S:1:2	S:2:1	S:2:2
S:1:1	$-21, 70.3°$	$-66.6, -77.9°$	$-0.0344, 65.5°$	$-69.9, -32.8°$
S:1:2	$-66.6, -77.9°$	$-21.1, 21.9°$	$-68.8, 28.8°$	$-0.0337, 110°$
S:2:1	$-0.0344, 65.5°$	$-68.8, 29.7°$	$-21, -119°$	$-66.8, 74.1°$
S:2:2	$-70, -31.8°$	$-0.0337, 110°$	$-66.8, 74.1°$	$-21.1, 17.6°$

5. MODE CONVERSION FROM TE10 TO TE10/TE20 OVER MODE

The converter to convert TE10 to TE10/TE20 modes is previously designed by Tantawi et al. [14]. This converter is shown in Figure 4.

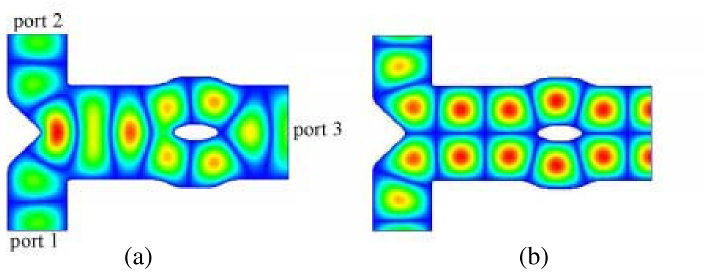

Figure 4. The assembly of TE10 to TE10/TE20 convertor, (a) the electric field of TE10 mode and (b) the electric field pattern of TE20 modes on the surfaces.

In this study, we adapt it to fit our design because our output rectangular waveguide port 3 has a different dimension. We design an adapter to match modes between two rectangular waveguides and attach it to the TE10 to TE10/TE20 convertor. The adapter utilizes a double arc geometry to ensure the smooth transition and full match at 11.424 GHz [15].

The waveguide geometry and electric field pattern on the surface are shown in Figure 5. The

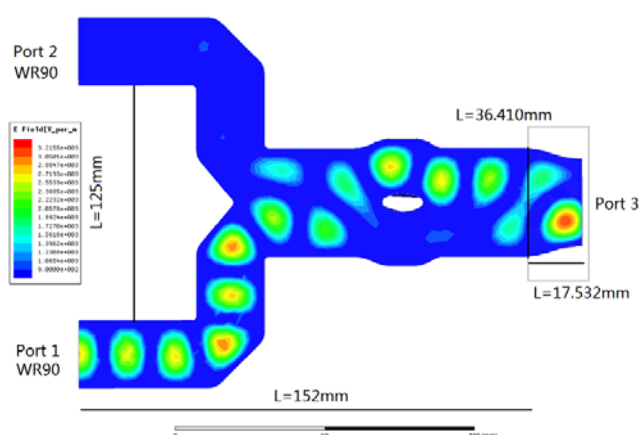

Figure 5. A snap shot of E field pattern on the mode converter. The input power on port 1 is 1 W. The dimensions are given. The double arc structure is shown in the gray frame.

optimized device can convert TE10 from port 1 into TE10/TE20 combination modes in port 3 without leakage to port 2. Ports 1 and 2 are standard WR90 waveguide, and port 3 has the same dimension as port 1 shown in Figure 3. Thus the two rectangular waveguides can be mounted together. The powers of TE10 and TE20 modes are equal on port 3 while port 1 and port 2 have a good isolation. To achieve these requirements, we numerically optimize the geometry of the center post island, waveguide taper adapter and protrusions on the left plate.

This end device has three ports and supports four modes. A 4 by 4 scattering matrix is used to check the mode conversion in Table 2. The result is from HFSS FEM simulation. From this matrix, the power from either port 1 or 2 will be equally split to TE10/20 on port 3. From Table 2, we can see that the powers are matched with little reflection from port 1 and port 3. Moreover, a good isolation occurs between port 1 and port 2.

Table 2. The scattering matrix of converter in Figure 11. The modes sequence is the same as shown in matrix 2. First two modes are TE10 in port 1 and 2 and the last two modes are TE10 and TE20 in port 3. $S : M : N$ means Nth mode on M port. First number is S parameter whose unit is decibel (dB) and second number is phase whose unit is degree.

Frequency:11.424GHz	S:1:1	S:2:1	S:3:1	S:3:2
S:1:1	$-31, 147°$	$-25.4, 95.5°$	$-3.0, 160°$	$-3.05, -111°$
S:2:1	$-25.4, 95.5°$	$-30.6, 129°$	$-3.03, -20.8°$	$-3.02, -112°$
S:3:1	$-3.0, 160°$	$-3.03, -20.8°$	$-28.4, -106°$	$-47.2, -7.51°$
S:3:2	$-3.05, -111°$	$-3.02, -112°$	$-37.6, -7.53°$	$-22.3, -153°$

6. ASSEMBLY OF THE SECOND OMT DESIGN

By cascading these two structures, the design of a X-band dual-polarization converter assembly is shown in Figure 6. This structure has three physical ports. Two are WR 90, and one is a circular waveguide. Figure 6 also shows the electric field at a snap shot. When the power input from one WR 90 rectangular waveguide is 1 W, the max E field on the surface is around 5800 V/m. The max field amplitude is directly proportional to the square root of the RF power amplitude. In this sense, the maximum E field on this device, when the input RF power is 50 MW, is 40.6 MV/m. It is less than the typical breakdown E field (200 mV/m) for X-band application [16, 17]. Therefore, this device will not have electric breakdown of arcing at 50 MW RF delivery.

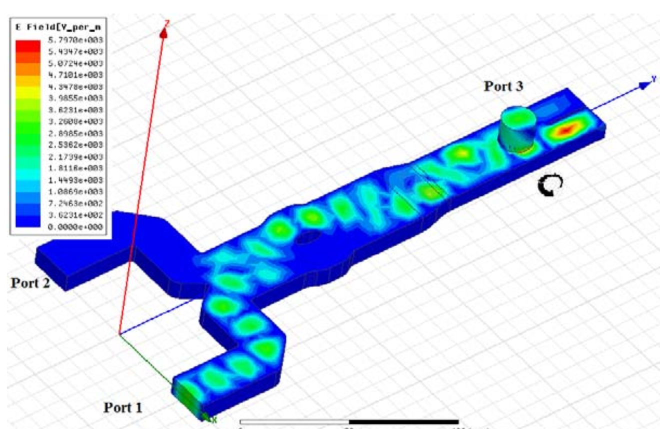

Figure 6. Final assembly of directional TE10 to dual polarizing circular converter and a snap shot of E field pattern is plotted when the input power on WR 90 is 1 W and max E field is less than 5.79 KV/m.

This device has three ports, and port 3 supports two modes. Thus a 4 by 4 scattering matrix is used to check the mode conversion in Table 3. This matrix matches matrix 2, and the power is converted to LHCP with little reflection and good isolation.

Table 3. The scattering matrix of second version in Figure 4. The modes sequence is the same as shown in matrix 2. First two modes are TE10 in port 1 and 2 and the last two modes are polarized TE11 in port 3. $S:M:N$ means Nth mode on M port. First number is S parameter whose unit is decibel (dB) and second number is phase whose unit is degree.

Frequency: 11.424 GHz	S:1:1	S:2:1	S:3:1	S:3:2
S:1:1	$-37.9, -57.3°$	$-45.6, 89°$	$-3, -21.4°$	$-3.02, 69.4°$
S:2:1	$-45.6, 89°$	$-35, -30.4°$	$-3.02, -21.6°$	$-3, -111°$
S:3:1	$-3, -21.4°$	$-3.02, -21.6°$	$-38.3, 159°$	$-47.1, 36.3°$
S:3:2	$-3.02, 69.4°$	$-3, -111°$	$-47.1, 36.3°$	$-34.6, 12.2°$

7. FREQUENCY RESPONSE, TRANSIENT RESPONSE AND THERMAL CONCERN

7.1. Frequency Response

The design of OMT convertors will be operated at 11.424 GHz, but it will be ideal to have a board frequency bandwidth. Considering that an X-band RF source can have an output bandwidth less than 1 MHz, this device will be suitable for accommodating the frequency shift and spread of those RF sources. The minimum bandwidth should be several megahertz. The scattering matrix elements and phase different are obtained as a function of frequency, and the results are illustrated in Figure 7. The left vertical axis is the scattering amplitude, and right vertical axis is the phase delay angle of two TE11 polarizations in a circular waveguide.

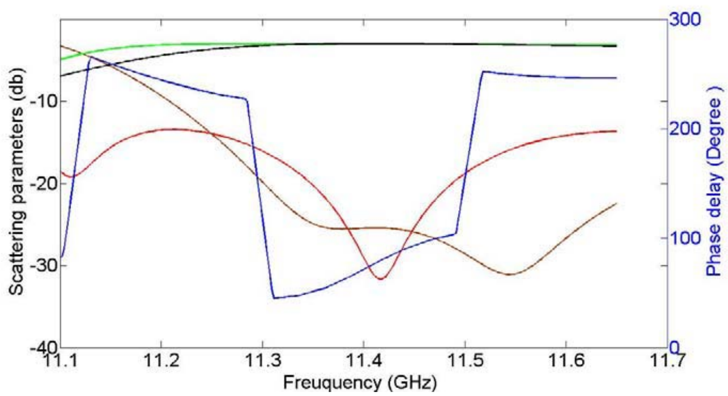

Figure 7. Frequency spectrum of the scattering parameter and phase difference of the dual polarizers. S parameters are plotted in color code. S(1,1:1,1) is red; S(2,1:1,1) is magenta; S(3,1:1,1) is greens; S(3,2:1,1) is black. Specifically, the phase delay is also plotted as function of frequency in blue. This phase delay bandwidth limits the bandwidth of this device.

First from prospective of amplitudes, this design will have 50 MHz bandwidth, if the isolation and reflection are required less than -25 db. On the other hand, the phase difference of two TE11 modes has a bandwidth only around 3 MHz for this design. Therefore, the total bandwidths of these OMT polarizers are 3 MHz to output circular polarization modes. These bandwidths are large enough for our RF source and OMT applications. We can adapt an elliptical phase corrector to further increase the bandwidth of correct phase delay. The bandwidth improvement research will be conducted in the future studies.

7.2. Thermal Concern

This converter is designed to convert multi-megawatts RF power into dual-polarization TE11 modes in the form of RHCP or LHCP modes in a circular waveguide. The converters will be machined from a single copper block to minimize the assembly error. The power loss on the surface can be non-trivial and should be estimated.

From the simulation, the main RF power loss concentrates on bottom of the circular waveguide where the magnetic fields are enhanced in Figure 8. To minimize the magnetic field, 1.5 mm radius blending chamfers are used to reduce the local H fields. In this simulation, we presume that the surface conductivity is 5.8×10^7 siemens/m. The RF loss on the surface of this design is calculated and simulated in HFSS e-physics, and plotted in Figure 6, and the integration loss is 0.0108 W when the input power is 1 W from a RF source. The total loss of each of the two devices is around 1% input RF power in a CW operation mode. Hence, this device will generate around 100 W RF surface loss on copper block when it delivers 1 MW pulsed RF power at 100 Hz repetition rate. Active chilling water pipes would lend enough capability to cool the whole system exterior around room temperature [18].

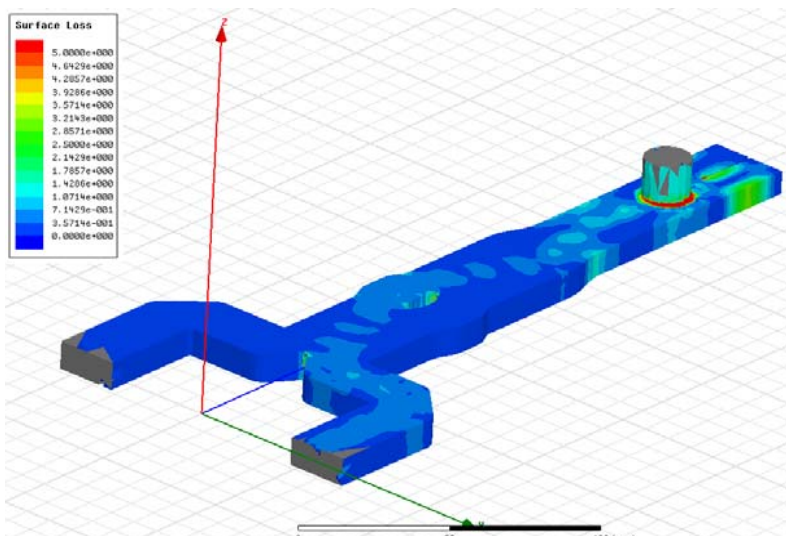

Figure 8. Schematic of surface RF loss density distribution for the dual polarizer at a steady state. The color code gives the guidance on the RF dynamic loss density.

8. CONCLUSION

We present two designs for X-band dual circular polarization transducers. The design uses all simple or existing shapes, and it will be easy to manufacture. This design has MHz operation bandwidth which is enough for our OMT application. This polarizer can be utilized for several motivations, including RHCP and LHCP signal broadcasting and receiving, high power RF loads and RF power compressors.

ACKNOWLEDGMENT

We would like to thank Dr. Chris Nantista from SLAC national accelerating laboratory for some useful discussions. This work was supported by the Department of Energy Contract No. DE-AC02-76SF00515.

REFERENCES

1. Kovac, M., E. M. Leitch, C. Pryke, J. E. Carlstrom, N. W. Halverson, and W. L. Holzapfel, "Detection of polarization in the cosmic microwave background using DASI," *Nature*, Vol. 420, 772–787, 2002.
2. Uher, J., J. Bornemann, and U. Rosenberg, *Waveguide Components for Antenna Feed Systems: Theory and CAD*, Artech House, Norwood, MA, 1993.
3. R. Ihmels, U. Papziner, and F. Arndt, "Field theory design of a corrugated septum omt," *IEEE MTT-S Int. Microwave Symp. Dig*, 909–912, 1993.
4. Virone, G., R. Tascone, M. Baralis, O. A. Peverini, A. Olivieri, and R. Orta, "A novel design tool for waveguide polarizers," *IEEE Trans. Microwave Theory Tech.*, Part 1, Vol. 53, No. 3, 888–894, Mar. 2005.
5. Zhong, W. Y., B. Li, Q. Y. Fan, and Z. Q. Shen, "X-band compact septum polarizer design," *ICMTCE*, 167–170, 2011.
6. Jung, Y. B., "Ka-band polariser structure and its antenna application," *Electronics Letters*, Vol. 45, 931–932, 2009.
7. Pisano, G., et al., "A broadband WR10 turnstile junction orthomode transducer," *IEEE Microwave and Wireless Components Letters*, Vol. 17, I 286, 2007.
8. Eisenhart, R. L., N. W. Nevils, J. J. Gulick, and R. C. Monzello, "A matched turnstile type 4-way divider/combiner," *IEEE Int. Microwave Symp. Dig.*, 166–168, 1983.
9. Aramaki, Y., N. Yoneda, M. Miyazaki, and T. Horie, "Ultra-thin broadband OMT with turnstile junction," *IEEE MTT-S Int. Dig.*, Vol. 1, 47–50, Jun. 2003.
10. Chang, C., S. Church, S. G. Tantawi, P. Voll, M. Sieth, and K. Devaraj, "Theory and experiment of a compact waveguide dual circular polarizer," *Progress In Electromagnetics Research*, Vol. 131, 211–225, 2012.
11. Chang, C., S. Tantawi, S. Church, J. Neilson, and P. V. Larkoski, "Novel compact waveguide dual circular polarizer," *Progress In Electromagnetics Research*, Vol. 136, 1–16, 2013.
12. Pozar, D. M., *Microwave Engineering*, 4th edition, Wiley, New York, USA, 2011.
13. HFSS, USA, http://www.ansys.com/.
14. Tantawi, S. G., C. Nantista, N. Kroll, Z. Li, R. Miller, R. Ruth, and P. Wilson, "Multimoded RF delay line distribution system for the next linear collider," *Phy. Rev. ST Accel. Beams*, Vol. 5, Iss. 032001, 2002.
15. Chen, X. and S. G. Tantawi, "Conceptual design of an ideal variable coupler for superconducting radiofrequency 1.3 GHz cavities," *Proceedings of International Particle Accelerator Conference*, 2648–2650, Dresden, Germany, 2014.
16. Wang, J., et al., "Fabrication technologies of the high gradient accelerator structures at 100 MV/m range," *Proceedings of International Particle Accelerator Conference*, 3819–3821, Kyoto, Japan, 2010.
17. Tantawi, S. G., C. D. Nantista, V. A. Dolgashev, C. Pearson, J. Nelson, K. Jobe, J. Chan, K. Fant, and J. Frisch, "High-power multimode X-band RF pulse compression system for future linear colliders," *Physical Review Special Topics — Accelerators and Beams*, Vol. 8, Iss. 042002, 2005.
18. Treml, C. A., S. K. Brown, and J. D. Bernardin, "Resonance control cooling system for a prototypecoupled cavity linac," *Proceeding of 8th International Conference on Accelerator & Large Experimental Physics Control Systems*, San Jose, California, US, 2001.